

FLOW IN SHALLOW RECTANGULAR BASINS: EXPERIMENTAL STUDY AND 2D NUMERICAL SIMULATIONS

Sameh Kantoush¹, Benjamin Dewals², Sébastien Erpicum³,
Anton Schleiss⁴ and Michel Piroton⁵

¹ Research associate, Laboratory of Hydraulic Constructions (LCH), Ecole Polytechnique Fédérale de Lausanne (EPFL), Station 18, CH-1015 Lausanne, Switzerland, e-mail: sameh.kantoush@epfl.ch

² Postdoctoral researchers, F.R.S.-FNRS and Group of Hydrology, Applied Hydrodynamics and Hydraulic Constructions, Department ArGENCo, University of Liege (ULg), Belgium, e-mail: b.dewals@ulg.ac.be

³ Research associate, Group of Hydrology, Applied Hydrodynamics and Hydraulic Constructions, Department ArGENCo, University of Liege (ULg), Belgium, e-mail: s.erpicum@ulg.ac.be

⁴ Professor, Laboratory of Hydraulic Constructions (LCH), Ecole Polytechnique Fédérale de Lausanne (EPFL), Station 18, CH-1015 Lausanne, Switzerland, e-mail: anton.schleiss@epfl.ch

⁵ Professor, Group of Hydrology, Applied Hydrodynamics and Hydraulic Constructions, Department ArGENCo, University of Liege (ULg), Belgium, e-mail: michel.piroton@ulg.ac.be

ABSTRACT

The planning and design of a sustainable reservoir require the accurate prediction of flow and sediment deposition patterns. Numerical simulation of flow in reservoirs is important in order to determine the detailed flow pattern. This typically includes flow separation at the inlet, accompanied by recirculation and stagnation regions. The aim of the present paper is to study the influence of the reservoir geometry on the flow patterns, by means of physical and numerical modelling of the flow behaviour. Different geometries were considered (characterized by different lengths of the basin), but with fixed inflow discharge and downstream water depth. In spite of the symmetric setup, leading to symmetric hydraulic and geometrical conditions, the physical and numerical experiments generally produced an asymmetric flow pattern that can easily switch sides depending on the initial and boundary conditions. The numerical simulations revealed that the observed asymmetry in flow patterns can be explained by the high sensitivity of the flow with respect to initial and boundary conditions. These numerical simulations succeed in predicting, with a satisfactory agreement compared to experiments, the influence of the length of the basin on the flow pattern.

Keywords: shallow flow, depth averaged model, reservoir geometry, reservoir hydrodynamic, flow instability, finite volume

1. INTRODUCTION

Background and objectives

Shallow flows can be defined as predominantly horizontal flows in a fluid domain where the vertical dimension is significantly smaller than the two horizontal dimensions. The instability of a two dimensional flow in a symmetric shallow reservoir with a suddenly expanded part is leading to large-scale transverse motions, as a result of the growth of transverse disturbances. It is important to understand such flows because of their prominence in nature and their practical importance in many applications, such as in sudden expansions Shapira (1998), jets and wakes Chen and Jirka (1997), in storage chambers Adamsson (2003) as well as in shallow reservoirs Kantoush (2005, 2006, 2007 and 2008). Moreover, these large-scale motions influence processes such as suspended sediment transport and thus are likely to affect bed deposition patterns.

Experimental observations of flows through a symmetric channel expansion are given by (Durst, 1974; Cherdron, 1978; John, 1984; and Sobey, 1985). The flow across an axisymmetric sudden expansion has all the complexities of an internally separating and reattaching flow. The large features of the axisymmetric sudden expansion flow, both laminar and turbulent, are fairly well known through flow visualizations and some quantitative studies (Durst, 1974; Fearn, 1990; Cherdron, 1978). A significant conclusion of these studies is that even if the geometry is symmetric, asymmetric flows develop under certain Reynolds number and geometric conditions. At low Reynolds numbers the flow remains symmetric with separation regions of equal length at each side of the expanding channel. The length of the separation regions increases with increasing Reynolds number. At higher Reynolds numbers, however, separation regions of unequal length develop and the asymmetry remains in the flow, even up to turbulent flow conditions. The conditions of asymmetry and the value of the transition critical Reynolds number have been reported in literature both experimentally and numerically. Mizushima and Shiotani (1996, 2001) have studied experimentally and numerically flow in symmetric channels with a suddenly expanded and contracted part for Reynolds numbers lower than 1500 in the approaching channel. The present study investigates flows with a considerably high Reynolds number of the order of 14,000.

A finite volume procedure was previously used by Battaglia (1997) for channels with sudden expansion only. Commercial CFD codes were employed by several authors, such as Adamsson (2003) or Kantoush (2005). In the present work, an upwind finite volume scheme, self-developed at the University of Liege (Dewals, 2006), is exploited in combination with an advanced depth-average $k-\varepsilon$ turbulence model of Erpicum (2006). This 2D numerical model leads to accurate results for the flow in a number of basin geometries and for various hydraulic conditions. The numerical results discussed have been carried out by the second author during his postdoctoral period at LCH, EPFL, Switzerland. Four experiments with clear water were performed in a recirculating large hydraulic installation (Kantoush, 2008). The effect of basin length was examined by reducing the length of the rectangular shallow basin from 6 m to 5, to 4, and to 3 m successively. This paper presents a series of experimental and numerical simulations with the objective of testing the sensitivity to different parameters in the numerical modelling. The influence of the basin geometry on the flow field has been investigated experimentally and numerically. Different options are analyzed, with a focus on the influence of the length of the basin. For each case, flow pattern comparison for the laboratory measurements and simulation results are shown. Simulations focus on the ability of the numerical model to predict the transition between stable and unstable configurations.

The numerical simulations have been performed by means of the flow model WOLF 2D solving the shallow-water equations (Dewals et al., 2006; Dewals, 2006) and developed at the University of Liege. The computational model is based on a finite volume approach and a Flux Vector Splitting technique, dealing with multiblock structured grids. Details about the model and the simulated results are given in Dewals et al. (2008).

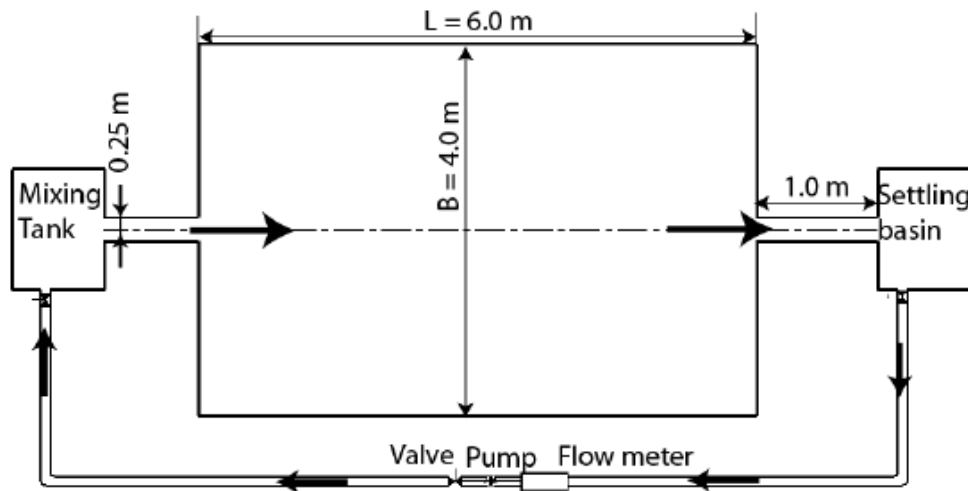
2. LARGE SHALLOW BASIN EXPERIMENTS

Laboratory experiments

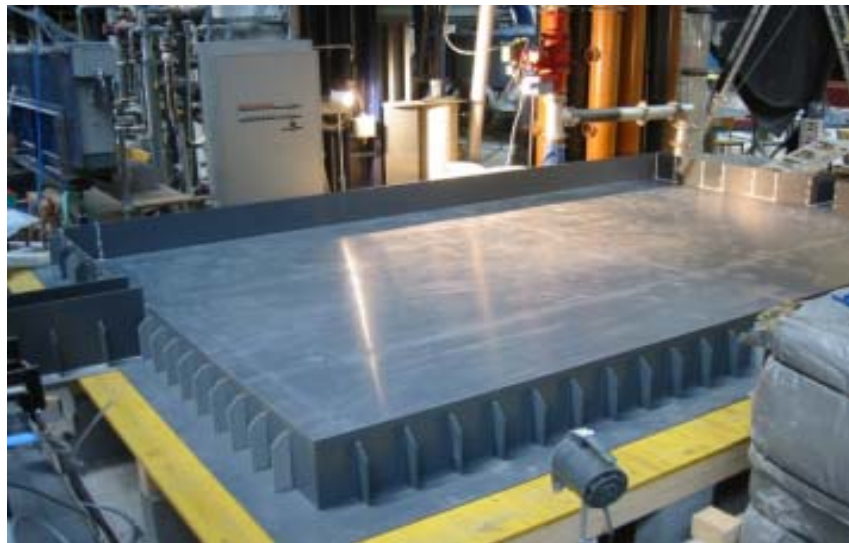
In the framework of a global research project dealing with the sedimentation of shallow reservoirs, reference rectangular basin geometry was studied in detail. The experimental tests have been conducted in a rectangular shallow basin with inner maximum dimensions of 6.0 m in length and 4m in width, as sketched in Figure 1. The inlet and outlet

rectangular channels are both 0.25 m wide and 1.0 m long. The bottom of the basin is flat and consists in hydraulically smooth PVC plates. The walls, also in PVC, can be moved to modify the geometry of the basin. Adjacent to the reservoir, a mixing tank is used to prepare the water-sediments mixture. The water-sediments mixture is supplied by gravity into the water-filled rectangular basin. Along the basin side walls, a 4.0 m long, movable frame is mounted to carry the measuring instruments.

The main measurement techniques employed include ultrasonic probes for measuring water levels, an Ultrasonic Velocity Profiler device (UVP) for measuring 3D velocity components as well as a Large Scale Particle Image Velocimetry technique (LSPIV) for measuring surface velocity fields Kantoush et al. (2008, 2006). More detailed description of the experimental setup and measurement equipment is provided by Kantoush (2008). The bed level evolution was measured with a Miniature echo sounder (UWS). The sounder was mounted on a movable frame which allows scanning the whole basin area. The sediment concentrations of the suspension material using the crushed walnut shells were measured. Two sensors SOLITAX sc were installed at the inlet and outlet channels for online suspended sediments measurements.



(a)



(b)




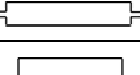
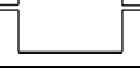



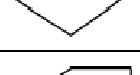
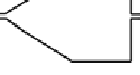
Figure 1: a) plan view of the experimental setup, b) photograph, looking downstream

The hydraulic conditions were chosen to fulfil the Froude similarity. Furthermore, for all tests, Froude number ($0.05 \leq Fr \leq 0.43$) was small enough and Reynolds number ($14000 \leq Re \leq 28000$) high enough to ensure subcritical, fully developed turbulent flow conditions.

Test configurations

Ten axi-symmetric basins with different forms were tested to study the geometry shape effect on the flow and deposition pattern (see Table 1). In order to gain insight into the physical process behind the sedimentation of shallow reservoirs governed by suspended sediment; a reference basin geometry with width of $B = 4.0$ m and length of $L = 6.0$ m was used. The reference geometry was used for the first six tests, from Test1 (T1) to Test6 (T6), to examine different test procedures and find the optimal one to continue with future test configurations. As a reference case, the rectangular basin geometry was analyzed in detail Kantoush (2008).

Table 1 Configurations of tested geometries and corresponding geometrical parameters.

Test	B [m]	L [m]	$AR = L/B [-]$	$ER = B/b [-]$	Form
T1, T2, T3, T4	4.0	6.0	1.5	16	
T7	3.0	6.0	2.0	12	
T8	2.0	6.0	3.0	8	
T9	1.0	6.0	6.0	4	
T11	4.0	5.0	1.25	16	
T12	4.0	4.0	1.0	16	
T13	4.0	3.0	0.75	16	
T14	4	6	1.5	8	
T15	4	6	1.5	16	
T16	4	6	1.5	12	

To investigate the effect of the basin width on the flow and sedimentation processes in the reservoir, a first series of experiments focused on the width have been conducted in the reservoirs of 6.0 m in length and 3.0, 2.0, 1.0 or 0.5 m in width (from T7 to T10), respectively. With a second set of experimental tests, the effect of the basin length has been investigated in rectangular shallow basins of 4.0 m in width and 5.0, 4.0 or 3.0 m in length (from T11 to T13), respectively. Finally geometries with three expansion angles were tested (from T14 to T16).

In the present paper only the results of flow pattern for different basin lengths (T1, T11, T12, and T13) are presented hereafter. The flow has been observed and analyzed for four different basin geometries. In all cases, the discharge is kept constant at $Q = 7.0$ l/s and the water level is controlled by a flap gate located in the downstream part of the outlet channel. The downstream water level was kept constant at $h = 0.2$ m.

In Table 1 dimensionless geometrical parameters are defined for the further analysis. The basin aspect ratio (AR), characterizing the geometry of the basin: $AR = L/B$ and the lateral expansion ratio (ER), characterizing the sudden enlargement at the transition between the inlet channel and the basin by $ER = B/b$.

3. Numerical modelling

WOLF 2D modelling system

Depth-averaged flow simulations representing the experimental set-up have been performed with the numerical model WOLF 2D, developed at the University of Liege and based on an original finite volume scheme (Dewals 2006, Erpicum 2006). The model is based on the two-dimensional depth-averaged equations of volume and momentum conservation, namely the “shallow-water” equations. In the “shallow-water” approach the basic assumption states that velocities normal to a main flow direction are smaller than those in this main flow direction. As a consequence the pressure field is found to be almost hydrostatic everywhere. The large majority of flows occurring in rivers, even highly transient, can reasonably be seen as shallow, except in the vicinity of some singularities. In the present study, measured vertical velocity components have been verified to remain low compared to velocity components in the horizontal plane. Therefore the flow in the basin may be considered as shallow and thus mainly two-dimensional (Kantoush et al., 2008).

Boundary conditions

The value of the specific discharge is prescribed as an inflow boundary condition. Besides, the transverse specific discharge is set to zero at the inflow. The outflow boundary condition is a constant water surface elevation: 0.2 m. At solid walls, the component of the specific discharge normal to the wall is set to zero. For the purpose of evaluating the diffusive terms, the gradients of the unknowns must also be specified at the boundaries. These gradients in the direction parallel to the boundary are set to zero for simplicity, while the gradients of the variables in the direction normal to the boundary are properly evaluated by finite difference between the value at the boundary and the value at the centre of the adjacent cell.

Ability of the model to represent the flow instability

A first simulation has been performed based on the initial and boundary conditions of the physical model of the rectangular geometry (T1). The algebraic turbulence model is used and the simulation is run until a steady-state flow field is reached. This obtained simulated flow field is perfectly symmetric (Fig. 2(a)). Although not in agreement with experimental

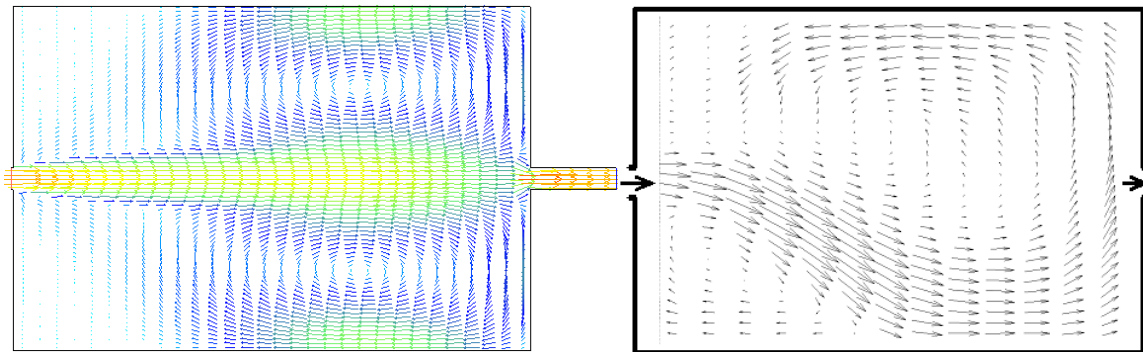
observations as shown in Figure 2(b), this result was expected since neither the mathematical model nor the algorithm implementation are supposed to break the perfect symmetry of input data. Consequently, this first simulation result demonstrates that the model does not include any spurious numerical artefact tending to introduce dissymmetry in a problem with perfectly symmetric input data. A non-symmetric solution could be obtained only with a non-symmetric initial flow field or with non-symmetric boundary conditions.

However, according to the laboratory experiments, this symmetric flow field is unstable. Therefore, a second series of simulations has been undertaken with slightly disturbed distributions of the specific discharge at the inflow, in order to test the stability of the numerical solution. Instead of being uniform, the cross-sectional profile of the specific discharge is specified with a linear variation along the width of the inlet channel:

$$q_{in}(y) = q_0 + q_1 \frac{2y}{b} \quad (1)$$

where q_{in} (m²/s) denotes the actual value specified as inflow boundary condition, q_0 (m²/s) is the reference value (total discharge divided by channel width) and q_1 (m²/s) measures the magnitude of the linear variation. b (m) designates the width of the inlet channel. As shown in Figure 4(a), considering this minor change in the inflow boundary condition with $q_1/q_0 = 2\%$ leads to a totally different flow field.

In order to verify that the simulated flow field does not significantly depend on the arbitrary value selected for the disturbance, five simulations have been run with q_1/q_0 varying between 1 % and 5 %. In every case, the flow field remains very close to that one observed at the laboratory (Figure 2(a)). For disturbance intensities between 1% and 5%, it is almost no effect on the simulated result.



(a) Numerical

(b) Experimental

Figure 2 Flow field simulated and measured with a uniform specific discharge profile

The artificial disturbance of the flow introduced here, through the non-uniform profile of specific discharge, represents actually unavoidable small disturbances existing in the experimental set-up. The slight perturbation of the inflow has a particularly strong effect on the results because of the unstable nature of the symmetric flow field.

As a consequence, it can be concluded that the numerical model is able to reproduce the high sensitivity of the real flow to external disturbances and hence the unstable nature of the symmetric solution in the present configuration. It has been verified that, even with a uniform specific discharge profile as inflow boundary conditions, similar simulation results can also be obtained by starting the computation with a flow field initially deviated. In this case, the non-symmetric initial condition acts as a disturbance.

4. Results and discussions

Experimental and numerical flow patterns

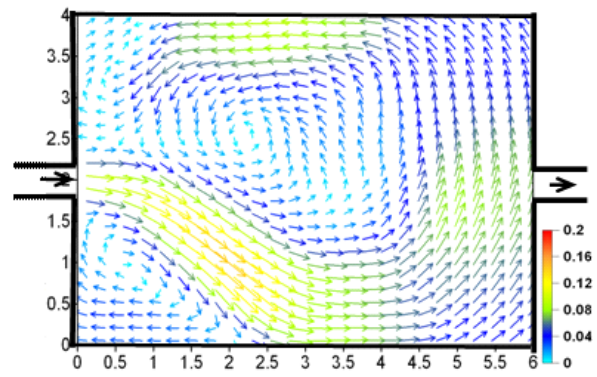
The asymmetric and symmetric behaviours of the flow are illustrated in Figures 3 (a) and (b) by Large-Scale Particle Image Velocimetry (LSPIV). Experimental results for a 4 m wide basin with lengths $L = 6$ and 5 m are shown. In spite of the symmetric setup, an asymmetric flow pattern is observed experimentally in Figure 3(a) where the basin length is higher than its width (6 m to 4 m).

The flow has an asymmetric behaviour, leading to a larger gyre size in the right upstream corner side than in the left side. The main gyre size is in accordance with the two corners gyres. The two corner gyres are depending from each other and alternatively change in size. Moreover, they control the size and location of the main gyre. The basin length has a strong influence on changing the flow field from an asymmetric flow to a stable symmetric flow. The experiments revealed a critical geometry shape factor, above which an initially symmetric flow evolves towards an asymmetric flow due to the Coanda effect. Figure 3(c) shows the second typical flow pattern, observed for shorter basin lengths. The flow remains essentially symmetric, with one circulation cell on each side of the centreline.

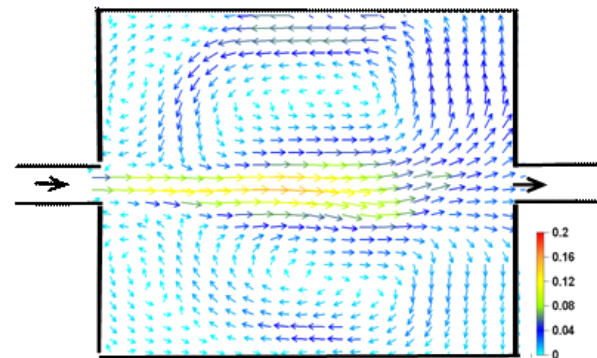
In spite of the symmetric setup, an asymmetric flow pattern is observed experimentally for T1 where the basin length is higher than its width. As can be noticed in Figure 3(a), the jet issuing from the inlet channel is considerably deviated in T1 and three large scale vortices develop, including a main large one rotating anticlockwise in the centre part of the basin. Furthermore, two smaller vortices rotating clockwise are formed in the upstream corners of the basin. The deflection of the jet can be explained by observing that a velocity increase on one side of the jet leads to a local reduced pressure, which in turn tends to amplify the asymmetry of the flow (Coanda effect, Chiang 2000). Simultaneously, in the deviated jet, an increase of the velocity leads to increased centrifugal forces, which tends to re-establish the symmetry of the flow pattern. A balance between those two effects is presumably reached in the steady state. The system tends to deviate alternatively to one side or to the other one, depending on slight disturbances existing in the initial and boundary conditions.

Figure 3(c) shows the second typical flow pattern, observed for shorter basin lengths. In the case of test T12, the flow remains essentially symmetric, with one circulation cell on each side of the centreline. As discussed previously, asymmetry disappears when the geometry aspect ratio AR , decreases. The symmetric and asymmetric behaviours of the flow are illustrated in Figure 3 by LSPIV results for 4 m wide basin with various lengths $L = 6, 5, 4$, and 3 m ($AR = 1.5, 1.25, 1$, and 0.75).

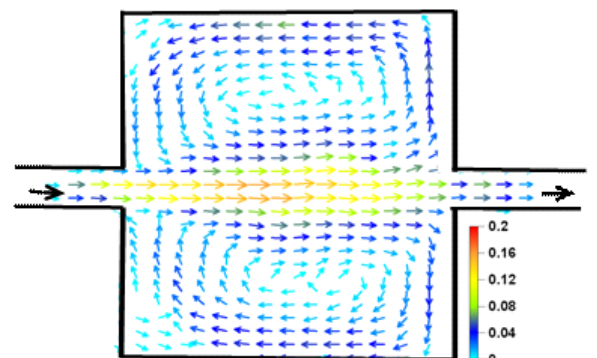
It can be seen that, for decreasing L and AR ratios, the flow is stabilized with a stable symmetrical pattern. Figure 3 on the left show the velocity vectors for various AR ratios with different lengths. The flow becomes more symmetric by decreasing distance from the inlet to the outlet, i.e. with decreasing length of the reservoir. Four vortices exist in the basin for an AR ratio of 1.25 as shown in Figure 3(b). The flow pattern becomes rather symmetric with respect to the centreline. The four gyres interact with the jet, which has some tendency to meander. The regions of the recirculating flow on the two sides of the basin centreline are identical in size, as shown in Figures 3(c) and 3(d). By comparing all basin lengths, it can be concluded that similar flow patterns have developed but with small differences regarding the dimensions and strength of the circulation cells.



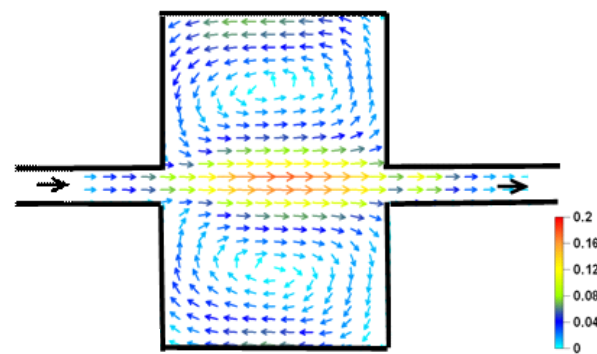
a)



b)

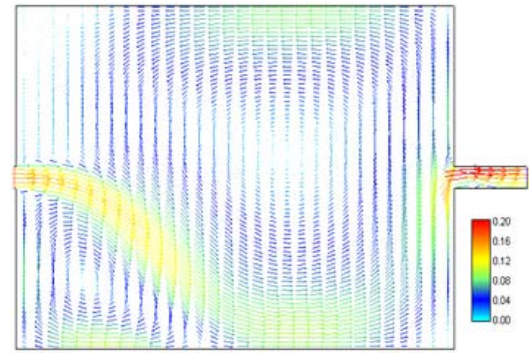


c)

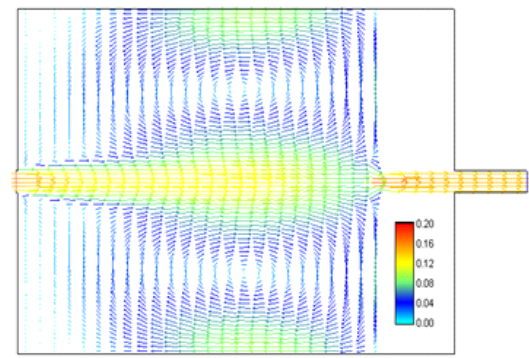


d)

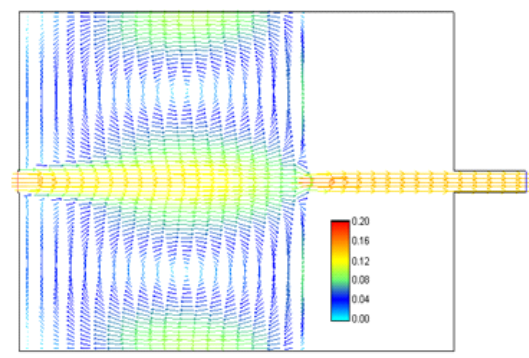
Figure 3: Measured average flow pattern with velocity vectors in a rectangular basin with a constant width of 4 m and four different lengths a) 6, b) 5, c) 4, d) 3m. Data obtained by LSPIV measurements. Velocity magnitude in m/s.



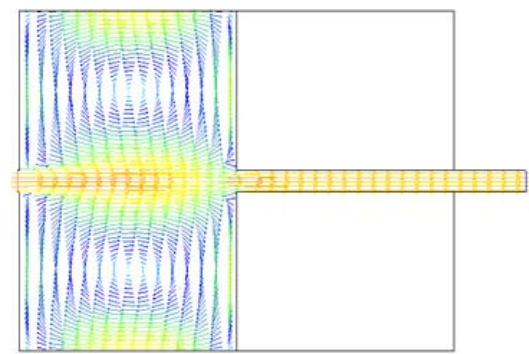
a)



b)



c)



d)

Figure 4: Simulated average flow pattern with velocity vectors in a rectangular basin with a constant width of 4 m and four different lengths a) 6 m, b) 5 m, c) 4 m, d) 3 m. Velocity magnitude in m/s.

Simulated

The output of the numerical model becomes now essentially consistent with experimental observations. Indeed, the deviation of the main jet is reproduced as shown in Figure 4(a). The three main vortices highlighted experimentally are also properly predicted by the numerical model. The slight perturbation introduced here has an amazingly strong effect on the results because of the unstable nature of the symmetric flow field. As a consequence, it can be concluded that the numerical model is able to reproduce the high sensitivity of the real flow to external disturbances and hence the unstable nature of the symmetric solution. It must be noted that identical simulation results can also be obtained, with a uniform specific discharge profile as inflow boundary conditions, by starting the computation with a flow field initially deviated. In this case, the non-symmetric initial condition acts as a disturbance Shapira *et al.* (1990).

Besides, the jet can be deviated either towards the right or towards the left side of the basin. In other words, two stable solutions exist and either of them can be obtained depending on the sign of q_1 or on the sense of the deviation in the initial condition. The occurrence of two distinct stable flow fields is also confirmed by the experimental tests (Kantoush 2006). The similar existence of multiple solutions was reported previously by other authors (Shapira *et al.*, 1990). The numerical model WOLF 2D is able to predict the transition between stable and unstable configurations. The stability of a symmetric flow field is analyzed by considering “quasi-symmetric” input data. Quasi-symmetric input data means symmetric geometry, symmetric outflow conditions and symmetric initial conditions, but slightly disturbed inflow boundary condition, according to relation (1). A geometric configuration is referred to as stable if a symmetric flow field remains stable for quasi-symmetric input data. On the contrary, the configuration is said to be unstable if, for quasi-symmetric input data, a symmetric flow field becomes unstable and the actual steady solution deviates considerably from the symmetric one. The last three configurations (Figure 4(b, c, d)) are found to permit a stable symmetric flow field, while the geometry shown in Figure 4(a) does not. This classification between stable and unstable configurations obtained from the 2D numerical simulations is in perfect agreement with experimental results as shown in Figure 3. Hence, it may be emphasized that the numerical model succeeds in reproducing the transition between basin lengths enabling a stable symmetric flow field and those leading to flow instability.

CONCLUSIONS

The experimental results are thus found to provide a means to capture the significant role of the geometry in the bifurcation process between asymmetric and symmetric flows.

Laboratory experiments and numerical simulations for a large rectangular shallow basin show that the basin geometry has a strong influence on the flow pattern. It is therefore highly depending on the boundary conditions, the initial flow conditions and the geometry.. Comparisons between experimental data and numerical results are presented. They demonstrate a reasonable agreement.

Although the simulations show that a 2D depth-averaged model already succeeds in reproducing the observed flow patterns in the laboratory, it is believed that future improvement of the modelling technique can lead to even more accurate predictions. For a better approximation of eddies and jets, a more detailed model for horizontal turbulence, such as LES (large eddy simulations) may be considered.

The present paper details numerical and experimental comparison of shallow flows in a series of rectangular basins for which experimental data is available. The experimental results include flow visualization for four different basin geometries (varying length of the basin). They show that, in spite of the geometrically and hydraulically symmetric setup with respect to the centreline of the basin, non-symmetric flow fields are observed for certain geometric and hydraulic conditions, while the flow field remains symmetric in narrower or shorter basins. For symmetric input data, the numerical model provides a perfectly symmetric result. However, if the inflow boundary condition is slightly disturbed, the numerical model performs well in reproducing both the symmetric and non symmetric flow patterns observed at the laboratory. On one hand, for the geometries corresponding to an observed non-symmetric flow field, the numerical model converges towards a completely deviated flow field, in very satisfactory agreement with laboratory measurements. The result is essentially insensitive to the arbitrary amplitude of the small disturbances superimposed to the inflow boundary condition.

Comparisons between experimental data and numerical results are presented. They demonstrate a reasonable agreement. On the other hand, for the geometries corresponding to an observed symmetric flow field, the slight disturbances introduced upstream are quickly damped and the computed steady flow field is found almost symmetric. Moreover, the numerical model accounts for wall roughness, which appears decisive for properly reproducing the third vortex, located in the upper part of the basin, in the case of non-symmetric flow fields. Consequently, the 2D simulations are found to reliably predict the influence of the length of the basin on the flow pattern or, in other words, the influence of the aspect ratio AR of the basin.

Although the simulations show that a 2D depth-averaged model can be used to reproduce the observed flow patterns in the laboratory, it is believed that future improvement of the modelling technique can lead to more still reliable predictions.

ACKNOWLEDGMENTS

The project is granted by the Swiss Federal Office for Water and Geology FOWG (now Federal Office for the Environment FOEN) in the framework of the project "Rhone-Thur - sustainable use of rivers".

The second author gratefully acknowledges the Belgian National Fund for Scientific Research (F.R.S.-FNRS) and the University of Liege (ARD and Duesberg Foundation), which provided funding for the numerical research carried out during his post-doctoral studies at the LCH-EPFL.

REFERENCES

- Adamsson, A., Stovin, V., and Bergdahl, L. (2003), Bed shear stress boundary condition for storage tank sedimentation, *J. Environ. Eng.-ASCE*, 129(7): 651-658.
- Battaglia, F., Tavener S.J., Kulkarni A.K. and Merkle C.L. (1997), Bifurcation of low Reynolds number flows in symmetric channels, *AIAA J*, 35:99-105
- Chen, D. and Jirka, G. (1997), Absolute and convective instabilities of plane turbulent wakes in a shallow water layer, *J Fluid Mech*, 338:157-172
- Chiang, T.P., Sheu, T.W.H., Wang, S.K. (2000), Side wall effects on the structure of laminar flow over a plane symmetric sudden expansion, *Comput Fluids*, 29:467-492.
- Cherdron, W., Durst, F., Whitelaw, J. H. (1978), Asymmetric flows and instabilities in symmetric ducts with sudden expansions, *J. of Fluid Mech.*, (84): 13 - 31.

- Dewals, B.J. (2006), Une approche unifiée pour la modélisation d'écoulements à surface libre, de leur effet érosif sur une structure et de leur interaction avec divers constituants, *PhD Thesis*, University of Liege, Liège, p 636.
- Dewals, B.J., Erpicum, S. Archambeau, P. Detrembleur, S. and Piroton, M. (2006), Depth-integrated flow modelling taking into account bottom curvature, *J. Hydraul. Res.* 44(6):787-795.
- Dewals, B. J., Kantoush, S. A., Erpicum, S., Piroton, M., and Schleiss, A. J. (2008), Analysis of flow instabilities in shallow rectangular basins, *Environmental Fluid Mechanics*, 8(1):31–54.
- Durst, F., Melling, A. and Whitelaw, J. (1974), Low Reynolds number flow over a plane symmetric sudden expansion, *J. of Fluid Mech.* (64) 111–128.
- Fearn, R., Mullin, T. and Cliffe, K. (1990), Nonlinear flow phenomena in a symmetric sudden expansion, *J. of Fluid Mech.* 211 Feb., 595–608.
- John, P. (1984), Plane sudden expansion flows and their stability, *Ph.D. thesis*, University of London.
- Kantoush, S. A., Bollaert, E., Boillat, J.L., and Schleiss. A. (2005), Suspended Load Transport in Shallow Reservoirs, *Proc. of 31st IAHR Biennial Congress*, Seoul, Korea.
- Kantoush, S. A., Bollaert, E.F.R., Boillat, J.-L., Schleiss, A.J. and Uijtewaal, W.S.J. (2006), Sedimentation Processes in Shallow reservoirs with different geometries, *Proc. Int. Conf. on Fluvial Hydraulics*, Lisboa, Portugal.
- Kantoush, S. A. (2007), Symmetric or asymmetric flow patterns in shallow rectangular basins with sediment transport, *In 32nd Congress of IAHR*, John F. Kennedy Student Competition, Venice, Italy.
- Kantoush, S. A., Boillat, J.-L., Bollaert, E., and Schleiss, A. (2008), Influence of shallow reservoir geometry on the flow pattern and sedimentation process by suspended sediments, *J. Wasser, energie, luft* 100(1): 13-21.
- Mizushima, J., Okamoto, H. and Yamaguchi, H. (1996), Stability of flow in a channel with a suddenly expanded part, *Phys. Fluids*. 8(11): 2933-2942.
- Mizushima, J. and Shiotani, Y. (2001), Transitions and instabilities of flow in a symmetric channel with a suddenly expanded and contracted part, *J. Fluid. Mech.*, (434):355-369.
- Shapira, M., Degani, D. and Weihs, D. (1990), Stability and existence of multiple solutions for viscous flow in suddenly enlarged channels, *Comput. Fluids*, 18(3): 239-258.
- Sobey, I. J. (1985), Observation of waves during oscillatory channel flow. *J. of Fluid Mech.* (151): 395–406.